Transactions of the Korean Nuclear Society Spring Meeting
Jeju, Korea, May 23-24, 2019

Extension of the SPACE Code Capability into Thermal-Hydraulic Analysis for Ocean Nuclear Reactor

Byoung Jae Kim [a*], Young Seock An[a], and Seung Wook Lee[b]
[a]*Department of Mechanical Engineering, Chungnam National University, 99 Daehak-ro, Yuseong-gu, Daejeon*
[b]*Thermal-Hydraluics and Severe Accident Research Division, Korea Atomic Energy Research Institute, Daejeon*
[*]*Corresponding author: bjkim@cnu.ac.kr*

1. Introduction

Various concepts have been proposed for ocean nuclear power plants with enhanced features [1-3]. The ocean nuclear reactor is characterized by the motion of the reactor system according to ocean environments. Thus, the thermal-hydraulic behavior must be investigated in the moving system.

Many efforts have been made to develop system codes for ocean nuclear power plants [4-7]. A domestic recent study also demonstrated the MARS code capability to predict flows under dynamic conditions [8].

The purpose of this study is to extend the SPACE code capability into thermal-hydraulic analysis for ocean nuclear reactor. This paper reports recent developments.

2. One-Dimensional Model

2.1 Governing Equations

It is well known that the governing equations for scalar properties remain unchanged under the change of frame. Thus, the forms of the two-fluid mass and energy equations are the same as those of existing equations. On the other hand, the two-fluid momentum equation is modified to account for fictitious forces.

$$\begin{aligned}&\frac{\partial}{\partial t}(\alpha_k\rho_k u_k)+\frac{\partial}{\partial x}(\alpha_k\rho_k u_k u_k)\\&=-\alpha_k\frac{\partial p}{\partial x}+F_{ik}+F_{wk}+u_k\Gamma_k \quad , \qquad (1)\\&+\alpha_k\rho_k(g_x-\ddot{R}_x)+\alpha_k\rho_k[\dot{\boldsymbol{\omega}}\times\mathbf{r}+\boldsymbol{\omega}\times(\boldsymbol{\omega}\times\mathbf{r})]_x\end{aligned}$$

where $\ddot{R}_x$ is the pipe direction component of the linear acceleration and $\boldsymbol{\omega}$ is the rotation vector.

2.2 Three-Dimensional Rotation Expression

The intrinsic rotation approach with Tait-Bryan angles was employed in this work. In Fig. 1, γ, β, and α are the rotation angles measured in the rotating coordinates. $\boldsymbol{\omega}$ and $\dot{\boldsymbol{\omega}}$ are functions of γ, β, and α such that

$$\begin{aligned}\boldsymbol{\omega}&=(\dot{\gamma}+\dot{\alpha}\sin\beta)\mathbf{i}\\&+(\dot{\beta}\cos\gamma-\dot{\alpha}\cos\beta\sin\gamma)\mathbf{j}\quad , \qquad (2)\\&+(\dot{\beta}\sin\gamma+\dot{\alpha}\cos\beta\cos\gamma)\mathbf{k}\end{aligned}$$

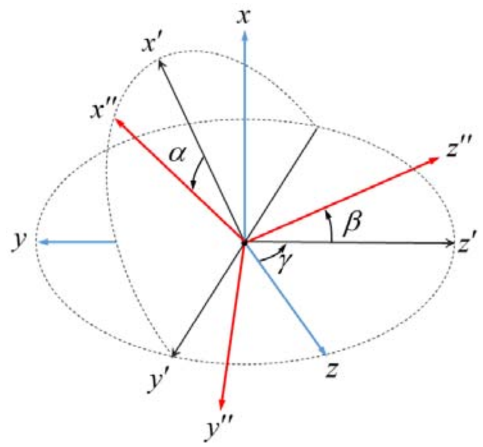

Fig. 1. Intrinsic rotation with Tait-Bryan angles

$$\begin{aligned}\dot{\boldsymbol{\omega}}&=(\ddot{\gamma}+\ddot{\alpha}\sin\beta+\dot{\alpha}\dot{\beta}\cos\beta)\mathbf{i}\\&+\begin{pmatrix}\ddot{\beta}\cos\gamma-\dot{\beta}\dot{\gamma}\sin\gamma-\ddot{\alpha}\cos\beta\sin\gamma\\+\dot{\alpha}\dot{\beta}\sin\beta\sin\gamma-\dot{\alpha}\dot{\gamma}\cos\beta\cos\gamma\end{pmatrix}\mathbf{j} \qquad (3)\\&+\begin{pmatrix}\ddot{\beta}\sin\gamma+\dot{\beta}\dot{\gamma}\cos\gamma+\ddot{\alpha}\cos\beta\cos\gamma\\-\dot{\alpha}\dot{\beta}\sin\beta\cos\gamma-\dot{\alpha}\dot{\gamma}\cos\beta\sin\gamma\end{pmatrix}\mathbf{k}\end{aligned}$$

where $\mathbf{i}$, $\mathbf{j}$, and $\mathbf{k}$ signify the unit vectors in the absolute coordinates. We need to express $\boldsymbol{\omega}$ and $\dot{\boldsymbol{\omega}}$ in terms of unit vectors in the moving coordinates because $\boldsymbol{\omega}$ and $\dot{\boldsymbol{\omega}}$ in Eq. (1) are vectors measured in the moving coordinates. The vector conversion between the absolute and moving coordinates is not difficult.

2.3 Thermal-Hydraulic and Component Models

The code must consider the dynamic change of the channel orientation. Therefore, the code was modified to update the geometric information such as inclination angle, azimuthal angle, elevation, etc. In addition, the options for hydrodynamic models were set to vary with time depending the channel orientation.

The hydrodynamic and heat transfer models must consider the effect of system oscillation. At this moment, they are not taken into consideration. The system inclination affects the separator performance [6]. The separator component will be improved in the future.

3. Result

2.1 Verification

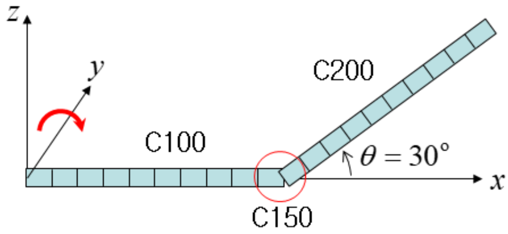

Fig. 2. *y*-axis rotation of connected pipes

Basic tests were performed to verify code modifications as intended. Figure 2 shows two connected pipes rotating about the *y* axis. The rotating speed is $\omega_y = (36t)^{\circ}$. Figures 3 ~ 6 show the variations of geometrical parameters of the two connected cells (C100-10 and C200-01). All parameters are predicted correctly. Figure 7 shows the dynamic change of the flow regime at cell C100-10 as the pipe rotates. Although not shown here, tests with rotations about *x* or *z* axis were also carried out. All geometrical parameters were correctly predicted.

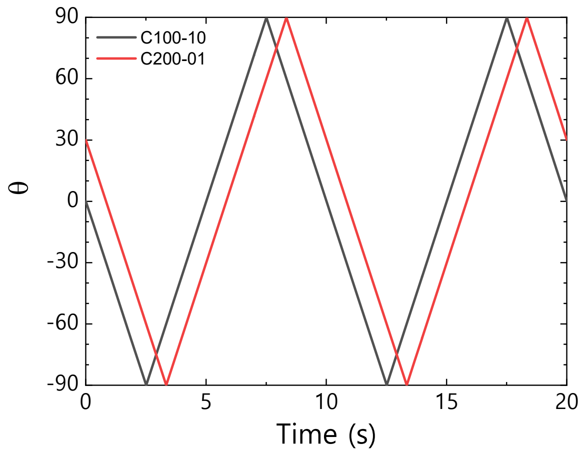

Fig. 3. Variations of the inclination angles (θ) of the two connected cells(C100-10, C200-01)

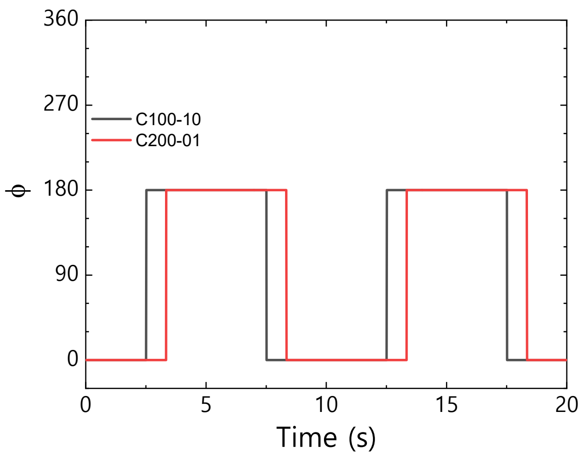

Fig. 4. Variation of the azimuthal angles (ϕ) of the two connected cells(C100-10, C200-01)

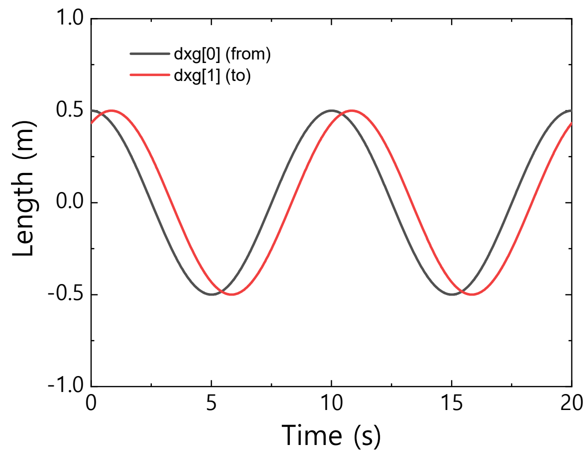

Fig. 5. Variations of the *x*-distances of the two connected cells(C100-10, C200-01)

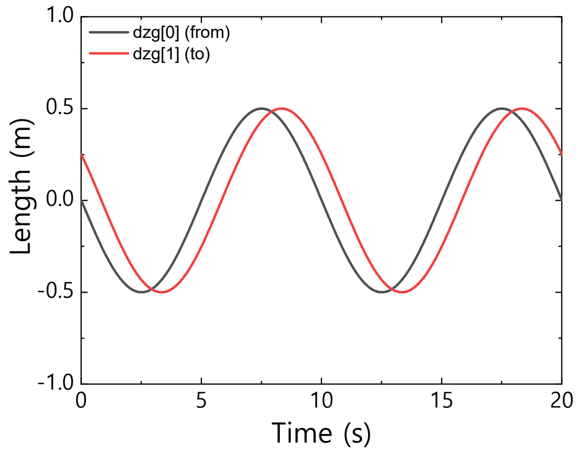

Fig. 6. Variations of the *z*-distances of the two connected cells(C100-10, C200-01)

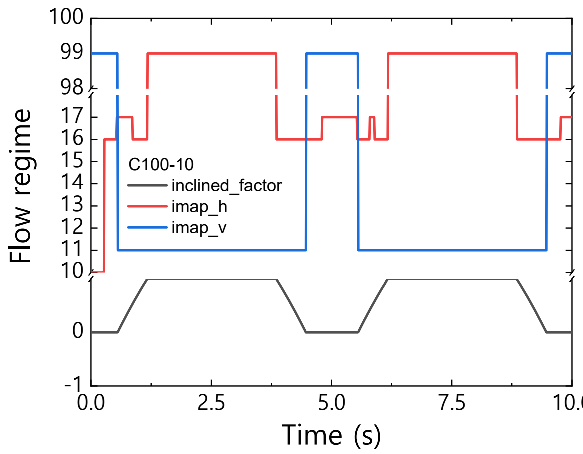

Fig. 7. Variations of flow regime map at cell C100-10

2.2 Rotating manometer

A conceptual test with manometer was performed. Figure 8 depicts the manometer half filled with water.

Figures 9~12 show the variation of the collapsed water level in each pipe with time. In Figs. 11, the manometer is rotated to the extent that the left pipe becomes empty and the right pipe is completely filled with water. On the whole, it is shown in Figs. 9~12 that the amount of water in each pipe is reasonably predicted.

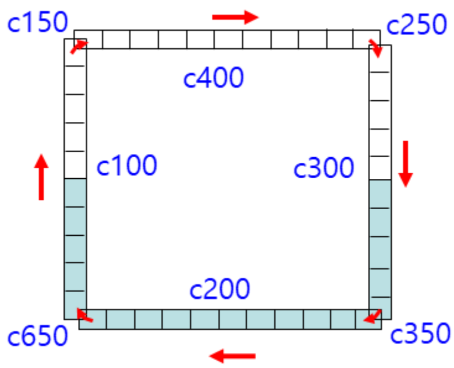

Fig. 8. Manometer

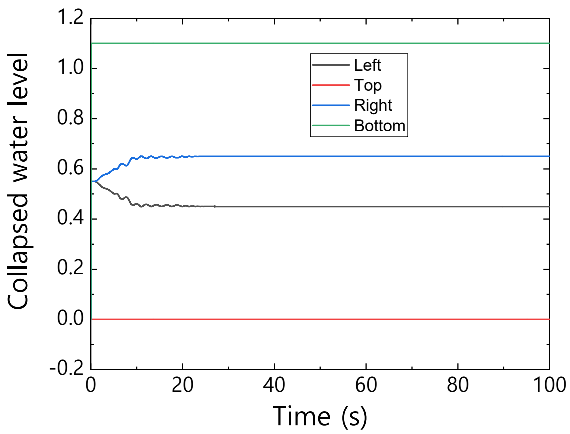

Fig. 9. Collapsed water levels when the manometer rotates clockwise by 10° for 10 s and stands still after 10 s.

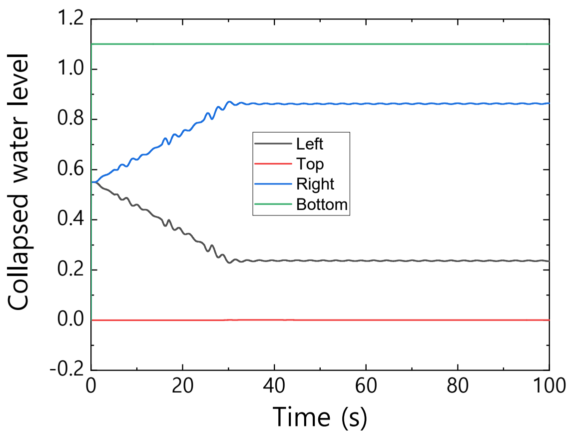

Fig. 10. Collapsed water levels when the manometer rotates clockwise by 30° for 30 s and stands still after 30 s.

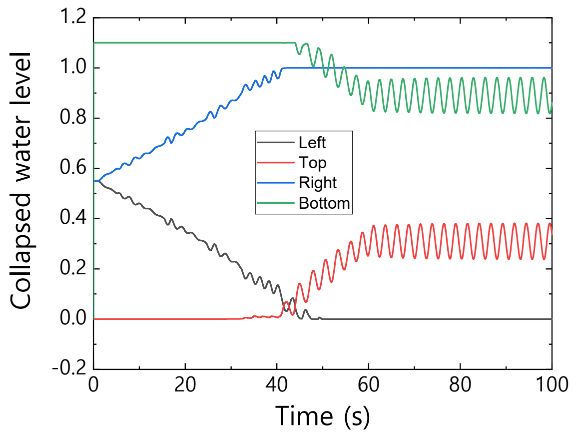

Fig. 11. Collapsed water levels when the manometer rotates clockwise by 60° for 60 s and stands still after 60 s.

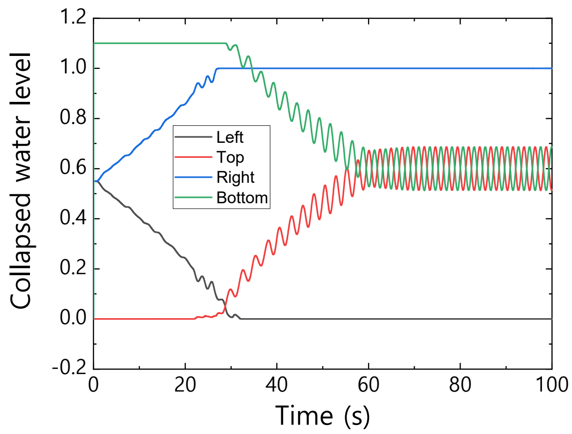

Fig. 12. Collapsed water levels when the manometer rotates clockwise by 90° for 60 s and stands still after 60 s.

3. Conclusions

The SPACE code has been improved to be equipped with simulation capability for ocean nuclear reactors. Basic tests showed that the geometrical parameters were correctly predicted as the pipes rotate. In addition, the flow motion was reasonably predicted in a rotating manometer. We are in the early development stage. Various conceptual and validation tests will be carried out.

ACKNOWLEDGEMENT

This work was supported by the National Research Foundation of Korea (NRF) funded by Ministry of Science and ICT (Grant No. NRF-2017M2A8A4016738).

REFERENCES

[1] J. Buongiorno, J. Jurewicz, M. Golay, N. Todreas, The Offshore Floating Nuclear Plant Concept, Nuclear Technology, 194(1) (2016) 1-14.
[2] K. Lee, K.-H. Lee, J.I. Lee, Y.H. Jeong, P.-S. Lee, A new design concept for offshore nuclear power plants with enhanced safety features, Nuclear Engineering and Design, 254 (2013) 129-141.
[3] K. Shirvan, R. Ballinger, J. Buongiorno, C. Forsberg, M. Kazimi, N. Todreas, Technology Selection for Offshore Underwater Small Modular Reactors, Nuclear Engineering and Technology, 48(6) (2016) 1303-1314.
[4] B.H. Yan, L. Yu, The development and validation of a thermal hydraulic code in rolling motion, Annals of Nuclear Energy, 38(8) (2011) 1728-1736.
[5] B.H. Yan, L. Yu, The experimental and theoretical analysis of a natural circulation system in rolling motion, Progress in Nuclear Energy, 54(1) (2012) 123-131.
[6] G.L. Mesina, D.L. Aumiller, F.X. Buschman, M.R. Kyle, Modeling Moving Systems with RELAP5-3D, Nuclear Science and Engineering, 182 (2016) 83-95.
[7] I. Ishida, T. Kusunoki, H. Murata, T. Yokomura, M. Kobayashi, H. Nariai, Thermal-hydraulic behavior of a marine reactor during oscillations, Nuclear Engineering and Design, 120(2–3) (1990) 213-225.
[8] H.K. Beom, G.W. Kim, G.C. Park, H.K. Cho, Verification of dynamic motion model for ocean condition in MARS using conceptual problems, in: Korean Nuclear Society Autumn Meeting, Gyeongju, Korea, 2017.